CHARACTERIZATION OF A RIGID BARRIER FILTER SYSTEM

Ta-Kuan Chiang
U.S. Department of Energy, National Energy Technology Laboratory
3610 Collins Ferry Road
P.O. Box 880
Morgantown, West Virginia 26507-0880, USA
ta-kuan.chiang@netl.doe.gov
Telephone 304-285-4406
Fax 304-285-4403

Abstract

A mathematical model is formulated to describe the dynamics of a rigid barrier filter system. Complete with filtration, regeneration and particle re-deposition, this model provides sizing information for new filter systems and diagnostic information for operating filter systems. To turn this model into a practical and smart filter system predictive model, monitoring devices for variables such as real-time particle concentration and size distribution are currently under laboratory development. The program goal is to introduce a smart filter system to supervise its operation and to assure its system reliability. Primarily, a smart filter system will update operating information, sound up malfunction alarms, and provide self-activated measures such as adjusting the cleaning frequency, intensity and back-pulse duration.

I. INTRODUCTION

The U.S. Department of Energy's (DOE) new approach for developing the technology needed for ultra-clean, 21st century energy plants is called "Vision 21". The goal of Vision 21 is to effectively remove, at competitive costs, environmental concerns associated with the use of fossil fuels for producing electricity, transportation fuels, and high-value chemicals. The program builds off of a suite of advanced technologies growing out of ongoing research and development (R&D) sponsored by DOE. As a vital part of the R&D program, efficient, reliable, and affordable particle filtration systems are essential for gasification-based plants using coal or solid fuel feedstock. The National Energy Technology Laboratory (NETL) has been investigating methods to characterize the operation of a rigid barrier filter system under high temperature and pressure applications. A mathematical model complete with filtration, regeneration and particle re-deposition is presented here to describe the dynamics of a rigid barrier filter system. This model can also be used to construct a computer-supervised smart filter system to warrant its system reliability. The required real-time monitoring devices are currently under laboratory investigation.

II. GENERAL DESCRIPTION OF A RIGID BARRIER FILTER SYSTEM

For high temperature and pressure particle filtration, most rigid filters investigated are candle filters having geometry of a candle. To withstand the high operating temperature and corrosive environment, candles are usually made of monolithic silicon carbide, composite oxide fibers, iron-aluminide or other alloy sintered and felted metals. Fig. 1 illustrates a typical high temperature and pressure rigid barrier filter system.

As shown in Fig. 1, the tube sheet physically separates the dirty and clean gas side. The incoming dirty gas passes through the candle filters which functionally separate the entrained particles, build up the filter cake and let clean gas past through. This particle filtration process goes on until that time when a limiting pressure drop is reached to initiate the filter regeneration. At the filter regeneration, a high-pressure back-pulse is introduced to dislodge the filter cake to recover the filter system pressure drop. Due to the short duration of the high-pressure back-pulse, of the order of a fraction of second, the dislodged filter cake if not settled out at the end of regeneration will be returned or re-deposited to the filter surface at the commence of following filtration cycle. Particle re-deposition of various degrees has been indeed observed for all rigid barrier filter systems. This unavoidable particle re-deposition however introduces an additional filter

system's pressure drop known as the residual pressure drop at the completion of filter regeneration. The entire filter system pressure drop, or the tube sheet pressure drop, under steady state operation, thus can be described to consist of three components: the conditioned filter element pressure drop, the residual pressure drop, and the filter cake pressure drop. A mathematical model complete with these three pressure drop components is presented below to describe the dynamic nature of a rigid barrier filter system including a tool to quantify the residual pressure drop.

III. RESIDUAL PRESSURE DROP FORMULATION

Nomenclatures:

ΔP_f	Filter system pressure drops, or tube sheet pressure drop
$\Delta P_{v\,f}$	Virgin filter pressure drop
ΔP_r	Residual pressure drop
ΔP_c	Fresh filter cake pressure drop
u_f	Face velocity
k_f	Virgin filter resistivity, defined as $k_f = \Delta P_{v\,f} / u_f$
K_2	Filter cake specific resistance coefficient
C	Particle concentration, weight/unit volume
t	Time element
T	Filtration period, duration of filtration before filter regeneration
γ	Fraction of dislodged filter cake re-deposited following filter regeneration, dimensionless
σ_f	Filter cake areal density, defined as $\sigma_f = C\, u_f\, t$
σ_r	Residual cake areal density, defined as $\sigma_r = \gamma\, \sigma_f$

A. Filter Regeneration at a Predetermined Time Interval

The overall filter system pressure drop, or the tube sheet pressure drop, is the sum of pressure drops of the virgin filter, the residual filter cake due to particle re-deposition, and the fresh filter cake. That is

$$\Delta P_f = \Delta P_{vf} + \Delta P_r + \Delta P_c$$

Start off at virgin filters, $\Delta P_r = 0$.

At face velocity of u_{f1}, particle concentration C_1 and filtration duration of t_1, the overall filter system pressure drop is

$$\Delta P_{f1} = k_f\, u_{f\,1} + K_{21}\, \sigma_f\, u_{f\,1} \qquad \textbf{(1)}$$

K_{21} indicates possible variations in particle size distributions.

At the end of filtration period t_1, filter regeneration begins. Unlike fabric filters, barrier filter regeneration is assumed to have all the residence filter cake been removed from its filter surface, re-entrained in the process flow stream and re-deposited γ_1 fraction of the filter cake back to the filter surface at the resumption of filtration again. The respective 1- γ_1 fraction is however removed from the process stream and actually settled out in the ash hopper. The re-deposited γ_1 fraction however forms the residual filter cake representing the residual filter pressure drop. Assuming this residual filter cake has the same specific resistance coefficient as the fresh filter cake, its pressure drop would then be

$$\Delta P_{r1} = \gamma_1\, (K_{21}\, \sigma_{f\,1})\, u_{f\,2} = K_{21}\, (\gamma_1\, \sigma_{f\,1})\, u_{f\,2} = K_{21}\, \sigma_{r1}\, u_{f\,2}$$

This completes the first filtration and regeneration cycle. Following the same reasoning, at face velocity u_{f2}, particle concentration C_2, and filtration period t_2, the total filter system pressure drop at the second filtration cycle is

$$\begin{aligned} \Delta p_{f\,2} &= k_f\, u_{f\,2} + K_{21}\, \sigma_{r\,1}\, u_{f\,2} + K_{22}\, \sigma_{f\,2}\, u_{f\,2} \\ &= k_f\, u_{f\,2} + K_{21}\, (\gamma_1\, \sigma_{f1})\, u_{f\,2} + K_{22}\, \sigma_{f\,2}\, u_{f\,2} \end{aligned} \qquad \textbf{(2)}$$

At the end of filtration period of t_2, the total filter cake is now

$$\sigma_{r1} + \sigma_{f\,2} = \gamma_1\, \sigma_{f\,1} + C_2\, u_{f\,2}\, t_2$$

Filter regeneration at a re-deposition fraction of γ_2 would produce a residual areal density of

$$\sigma_{r\,2} = \gamma_2\, (\sigma_{r\,1} + \sigma_{f\,2}) = \gamma_2\, \gamma_1\, (\sigma_{f\,1}) + \gamma_2\, (\sigma_{f\,2})$$

Similarly, following the same approach in deriving Eq. (2), it can be seen that at face velocity $u_{f\,3}$, particle concentration C_3, and filtration period t_3, the total filter system pressure drop at the third filtration cycle is

$$\begin{aligned} \Delta p_{f\,3} &= k_f\, u_{f\,3} + K_{22}\, \sigma_{r2}\, u_{f\,3} + K_{23}\, \sigma_{f\,3}\, u_{f\,3} \\ &= k_f\, u_{f\,3} + K_{22}\, [\gamma_2\, \gamma_1\, (\sigma_{f\,1}) + \gamma_2\, (\sigma_{f\,2})]\, u_{f\,3} + K_{23}\, \sigma_{f\,3}\, u_{f\,3} \end{aligned} \qquad \textbf{(3)}$$

It is now apparent that at the nth filtration cycle at face velocity $u_{f\,n}$, particle concentration C_n , and filtration period t_n, the total filter system pressure drop at steady state is

$$\begin{aligned}\Delta p_{f\,n} &= k_f\ u_{f\,n} + K_{2\,(n-1)}\ \sigma_{r\,(n-1)}\ u_{f\,n} + K_{2\,n}\ \sigma_{f\,n}\ u_{f\,n} \\ &= k_f\ u_{f\,n} + K_{2\,(n-1)}\ [\gamma_{n-1}\ \gamma_{n-2}\ \gamma_1\ (\sigma_{f\,1}) + \gamma_{n-2}\ \gamma_{n-3}\ \gamma_1\ (\sigma_{f\,2}) + \cdots \\ &\qquad + \gamma_{n-1}\ (\sigma_{f\,(n-1)})]\ u_{f\,n} + K_{2\,n}\ \sigma_{f\,n}\ u_{f\,n} \end{aligned} \quad \textbf{(4)}$$

B. Generalization

For constant particle concentration C, constant specific resistance coefficient K_2, constant face velocity u_f , predetermined filtration period T and constant re-deposition rate γ, Eq. (4) reduces to

$$\begin{aligned}\Delta p_{f\,n} &= k_f\ u_f + K_2\ \sigma_{r\,(n-1)}\ u_f + K_2\ \sigma_f\ u_f \\ &= k_f\ u_f + K_2\ (\gamma^{n-1} + \gamma^{n-2} + \cdots + \gamma^2 + \gamma)\ \sigma_f\ u_f + K_2\ \sigma_f\ u_f \end{aligned} \quad \textbf{(5)}$$

For $\gamma \neq 1$, the geometric series in the parenthesis converges when the filter system reaches its steady state. Eq. (5) reduces to

$$\begin{aligned}\Delta p_{f\,n} &= k_f\ u_f + K_2\ [\gamma/(1-\gamma)]\ \sigma_f\ u_f + K_2\ \sigma_f\ u_f \\ &= k_f\ u_f + K_2\ [\gamma/(1-\gamma)]\ C(u_f)^2\ T + K_2\ C(u_f)^2\ T \end{aligned} \quad \textbf{(6)}$$

From the observed filter system pressure drop versus time characteristics, the maxim tube sheet pressure drop at T according to Eq. (6) is

$$\Delta P_{f\,n\,(max)} = k_f\ u_f + K_2\ [\gamma/(1-\gamma)]\ C(u_f)^2\ T + K_2\ C(u_f)^2\ T \quad \textbf{(7)}$$

After filter regeneration, the minimum tube sheet pressure drop according to Eq, (6) is

$$\Delta P_{f\,n\,(min)} = k_f\ u_f + K_2\ [\gamma/(1-\gamma)]\ C(u_f)^2\ T \quad \textbf{(8)}$$

Taking the difference of Eq. (7) and Eq. (8),

$$\Delta P_{f\,n\,(max)} - \Delta P_{f\,n\,(min)} = K_2\ C(u_f)^2\ T \quad \textbf{(9)}$$

Also, from Eq. (8), we have

$$\gamma/(1-\gamma) = (\Delta P_{f\,n\,(min)} - \Delta P_{vf}) / [\ K_2\ C(u_f)^2\ T\ ] \quad \textbf{(10)}$$

Solving Eqs. (9) and (10), the re-deposition fraction γ reduces to experimentally observable quantities. The re-deposition fraction γ is

$$\gamma = (\Delta P_{f\,n\,(min)} - \Delta P_{vf}) / (\Delta P_{f\,n\,(max)} - \Delta P_{vf}) \quad \textbf{(11)}$$

For varying particle concentration C, varying specific resistance coefficient K_2, varying face velocity u_f , and varying filtration period T, the re-deposition fraction γ is best followed by a real time data acquisition system.

In fact, rigid barrier filters are not absolute filters. Virgin filters after use quickly reach their conditioned steady state having different but higher pressure-drop characteristics than its virgin state due primarily to the fine particles trapped within the filter element. Therefore, ΔP_{vf} in Eq. (11) needs be substituted with the conditioned steady state pressure drops.

III. DISCUSSIONS

Following Eqs. (1) to (4), a spread sheet program can be written to track down the dynamic nature of a rigid barrier filter system operation. Fig. 2 illustrates typical filter system pressure drop versus time characteristics separating pressurized fluid-bed combustion (PFBC) particles under varying face velocities. This figure also shows different degrees of re-deposition at various face velocities. Change of particle characteristics will significantly change the filter system operating characteristics. To assure a reliable filter system operation to positively protect its downstream gas turbine, continuous real time particle monitoring are essential to provide information on particle concentration and particle size distribution both at the filter system inlet and outlet. The inlet particle concentration provides information to extract the numerical filter cake specific resistance coefficient from the slope of the filter pressure drop characteristics. The inlet particle size distribution provides additional information on filter cake as related to increasing slope of the filter pressure drop characteristics, ineffective filter regeneration, and undesirable degree of particle re-deposition. The outlet particle concentration and size distribution provide information to meet the environmental regulation and the gas turbine protection requirement. Currently, a light scattering particle-monitoring device is setup in NETL High-Temperature Gas-Stream Cleanup Test Facility for evaluation. Successful completion of this evaluation would

lead to an ultimate computer-supervised smart filter system to supervise the high-temperature high-pressure filter system operation and to assure the system reliability. It is anticipated that a smart filter system will provide operating information update, malfunctioning alarms, and self-activated measures such as adjusting the cleaning frequency, intensity and back-pulse duration.

CONTRIBUTING AUTHORS: **ERIK M. SAAB, PAUL C. YUE, GARY F. McDANIEL, KARL H. WARNICK**
U.S. Department of Energy, National Energy Technology Laboratory
3610 Collins ferry Road
P.O. Box 880
Morgantown, West Virginia 26507-0880, USA

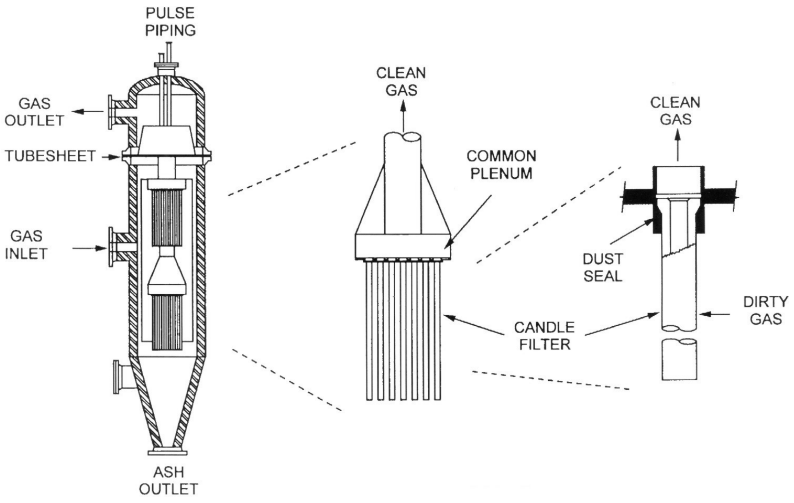

Figure 1. Typical rigid barrier filter system for high-temperature high-pressure applications

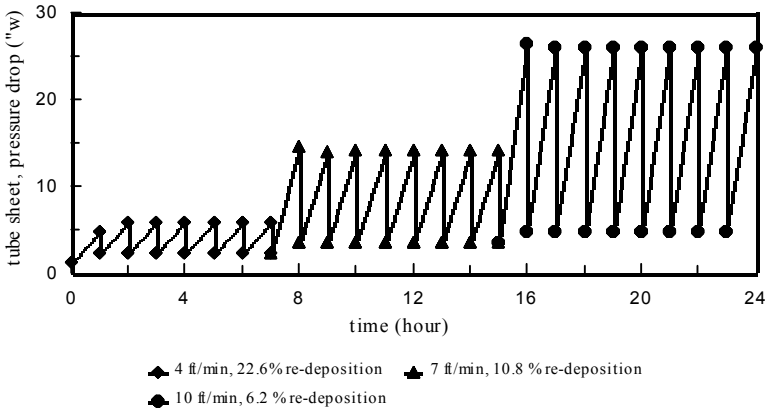

Figure 2. Typical rigid barrier filter system pressure-drop characteristics:
Feltmetal candle filter, 1.5mlong x 60mm o.d.
PFBC Tidd-Brilliant Demonstration Plant flyash.
1500 deg. F., 150 psig, 3000 ppmw particle loading.
Tube sheet pressure drop <2.5 psi (69"-w).
Optimized regeneration: dislodged cake size = filter cake thickness.